Interpretation of Particle Fouling in Submerged Membrane Filtration by Blocking Models

Kuo-Jen Hwang* and Fung-Fu Chen

Department of Chemical and Materials Engineering, Tamkang University, Tamsui, Taiwan 251, R.O.C.

Abstract

The particle fouling in a submerged membrane filtration system is analyzed by use of membrane blocking models. Two kinds of ceramic membranes made of ZrO_2-TiO_2, K-04 and K-06, are used in experiments. Their mean pore sizes on the outer surfaces are 8 and 5 μm, respectively. The values of blocking index under various filtration pressures are calculated and discussed. At the initial period of a filtration, the membrane internal blocking is dominant, and the blocking index decreases quickly. The index then suddenly drops to zero at a critical condition and keeps invariably thereafter. The boundary between membrane blocking and particle bridging conditions can be grasped by this blocking index analysis. Membrane blocking occurs only under higher filtration flux or less particle accumulation, while a filter cake may be formed to the contrary conditions. To compare the filtration performances of used membranes, membrane K-04 results in more severe membrane blocking at the initial period of filtration because of more large nominal pores. However, more particles can be continuously held up in the large pores of membrane K-06 due to a little wider pore size distribution and its higher internal porosity. This study provides a useful method to understand the variation of each filtration resistance source during filtration. An increase in filtration pressure leads both resistances due to membrane blocking and cake formation to be increased, as a result, causes to a decrease in the filtration flux. The agreement between calculated filtration resistances and experimental data demonstrates the reliability of the proposed method.

***Key Words*:** Membrane Filtration, Particle Fouling, Microfiltration, Blocking Models, Filtration Resistance

1. Introduction

Submerged membrane filtration has been increasingly applied to concentrate microbial cells in bioreactors or to produce clean water in wastewater treatments in recent years. In these operations, particle fouling on the membrane surface or blocking in the membrane pores may cause to a rapidly decline in filtration flux, as well as to the major difficulty on keeping a high performance.

In the past thirty years, many models or theories have been proposed for relating the steady filtration flux and operating conditions in microfiltration. For example, the concentration polarization models were commonly used in the conditions which diffusion- and convection- mass transfers were both dominant [1]. The hydrodynamic models were frequently applied in the condition which a filter cake was formed on the membrane surface. The migration and deposition of particles were analyzed based on hydrodynamics [2,3]. On the other hand, the blocking models were employed to analyze how and when the membrane pores were blocked by fine particles [4,5].

According to the analysis of Hermia [4], the blocking models can be expressed by a unique equation relating filtration time, t, and received filtrate volume per unit area, v, that is,

*Corresponding author. E-mail: kjhwang@mail.tku.edu.tw

$$\frac{d^2t}{dv^2} = K\left(\frac{dt}{dv}\right)^i \quad (1)$$

where K is the resistance coefficient while i is the blocking index. These parameters are functions of blocking modes, e.g., $i = 2$ for a complete blocking, $i = 1.5$ for a standard blocking, $i = 1$ for an intermediate blocking, and $i = 0$ for the cake filtration [4]. These blocking modes might change from one to another during a microfiltration [5–7]. Hwang and Lin [6] indicated that different membrane morphologies caused to different blocking modes at the initial stage of filtration, and the blocking modes changed to the cake filtration mode after a period of time whatever the kinds of membranes used. The effects of surface morphology and pore structure of membranes on the initial rate of protein fouling were studied by Ho and Zydney [5] using blocking models. The variations of blocking index were illustrated by scanning electron microscope (SEM). They also developed a combined pore blockage and cake filtration model for the fouling of protein aggregates during microfiltration [8]. Their models provided a smooth transition instead of a step change from pore blockage to cake filtration. Recently, Hwang et al. [9] established a blocking chart for track-etched membrane to relate the blocking index, filtration flux and particle accumulation. Once the resistance coefficient in Hermia's equation was related to the blocking index by regressing experimental data, the filtration flux during a microfiltration could be simulated accurately based on the blocking chart and the blocking models.

In this study, the blocking models are employed to explain the particle fouling in submerged membrane filtration using different ceramic membranes. The effects of filtration pressure and membrane pore size distribution on the blocking index and filtration resistances are discussed thoroughly.

2. Materials and Methods

A spherical particulate sample made of polymethly methacrylate (PMMA) and manufactured by Soken Co. in Japan (Cat. No. MX-500) was filtered in experiments. The particles have a sharp size distribution and a mean diameter of 5.0 μm. The particles were suspended in deionized water to prepare a 0.1 wt% suspension. The pH and temperature of the suspension were kept at 7.0 and 20 °C, respectively. The zeta potential of particles in such a condition was measured as -20 mV using a zeta sizer of *Malvern* 4700. Since the particles had a density of 1190 kg/m^3 and a hydrophilic surface, they could be suspended stably. Two hydrophilic ceramic membranes manufactured by Orelis Co. in France, *Kerasep* #06040 (K-06) and *Kerasep* #04040 (K-04), were used in experiments as the filter media. Both of them were made of ZrO_2-TiO_2, and these cylindrical ceramic membranes had the same dimensions, an inner diameter of 6.0×10^{-3} m, an outer diameter of 1.0×10^{-2} m, and a length of 4.0×10^{-1} m. The structures of their outer surfaces were imaged by a Scanning Electron Microscopy and the nominal pore size distributions were then analyzed by a *Power Image Analysis System* designed by Ching-Hsing Co. in Taiwan. The size distributions are shown in Figure 1. It can be found that the mean pore sizes for membranes K-06 and K-04 were ca 5 μm and 8 μm, respectively. Although membrane K-06 had a smaller pore size distribution, it exhibited a lower clean membrane resistance. This can be inferred that membrane K-06 had a higher internal porosity from the well-known "Kozeny-Carman equation" for fluid flow through porous media.

A schematic diagram of the submerged membrane filtration system is shown in Figure 2. The particles were suspended uniformly in an 80-liter suspension tank by a mechanical mixer. The filtration pressure was supplied by a vacuum pump. Membrane filtration experiments

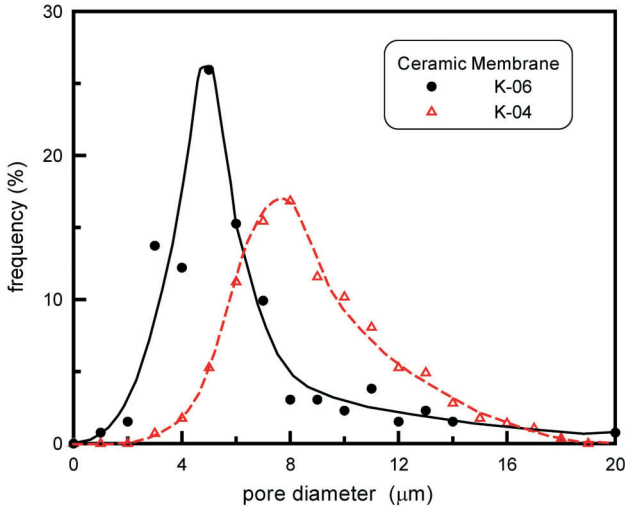

Figure 1. The pore size distributions of two used ceramic membranes.

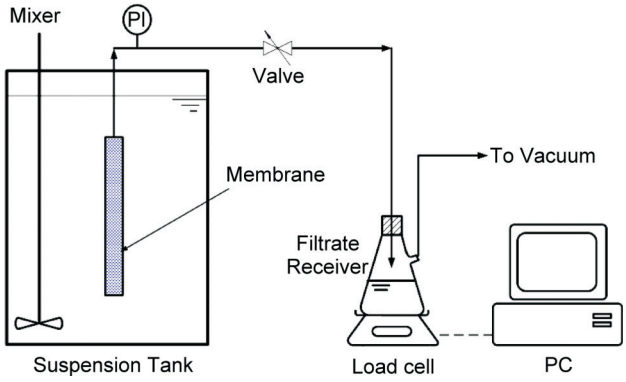

Figure 2. A schematic diagram of the submerged membrane filtration system.

under various constant pressures were carried out in an outside-in scheme. The instantaneous filtrate weight was detected by a load cell and recorded in a personal computer during filtration. Therefore, the filtration data of received filtrate volume versus time under various filtration pressures by using two different membranes were obtained.

3. Results and Discussion

Figure 3 shows the attenuation of filtration flux during submerged membrane filtration using two different membranes. The filtration pressures were kept at 40 kPa. At the beginning of filtration, the flux for membrane K-06 is much higher than that for K-04 because of the lower clean membrane resistance. However, the higher flux may cause the coming particles to have more opportunities to migrate into membrane pores to result in an internal pore blocking. The filtration flux of membrane K-06 then attenuates very quickly at the initial period. The flux decays for these two membranes become slower after 4,000 s due to the slowing down of particle fouling. Figure 4 shows the effects of filtration pressure and membrane type on the filtration flux at 10,000 s. Although the filtration driving force is increased by increasing filtration pressure, an unexpected decrease in filtration flux is found. This phenomenon is more significant for the membrane with a larger pore size distribution, e.g., more large pores for membrane K-04. It reveals that the filtration resistance due to membrane fouling increases markedly with filtration pressure; and that increasing filtration pressure is, of course, not an efficient method to enhance filtration flux in the condition of this study. Since a smaller pore size is harder to occur an internal blocking at the initial stage of filtration, a higher flux can be obtained for the membrane K-06 within the operating conditions of this study. In order to understand the roles of cake formation and membrane blocking on the performance of submerged membrane filtration using membranes with different pore size distributions, the blocking models were employed to analyze the blocking index as follows.

Figure 5 shows the filtration curves of dt/dv versus v for K-04 membrane under three different filtration pressures. The values of received filtrate volume, v, and filtration time, t, were measured in experiments. According to the conventional filtration theory, the filtration curve can be regressed to a straight line if the average specific filtration resistance of cake is constant and no membrane blocking occurs [9]. However, each curve shown in the

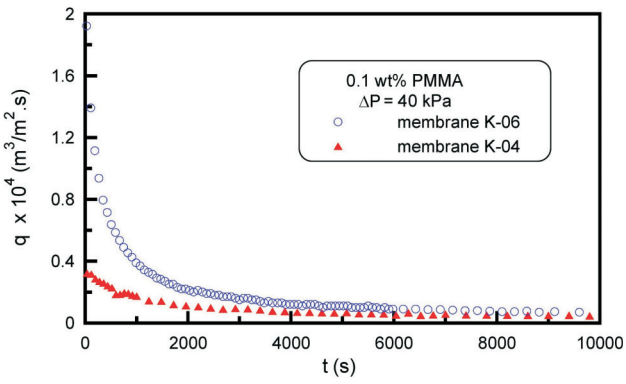

Figure 3. The time courses of filtration flux during microfiltration using two different membranes under a fixed filtration pressure.

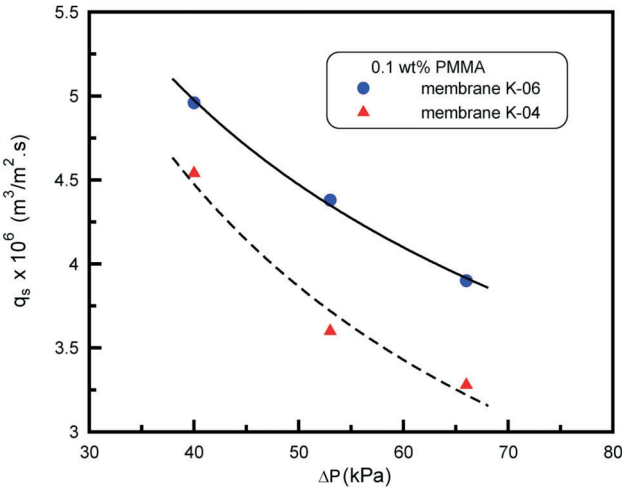

Figure 4. Effect of filtration pressure on the filtration flux at 10,000 s for two membranes.

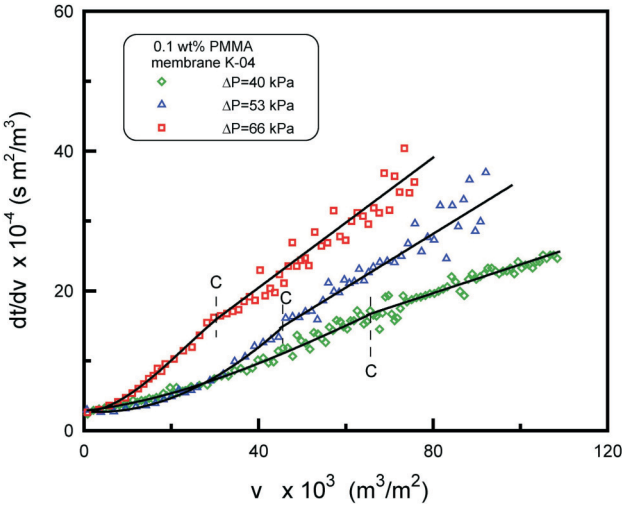

Figure 5. The filtration curves of dt/dv versus v under three different filtration pressures for membrane K-04.

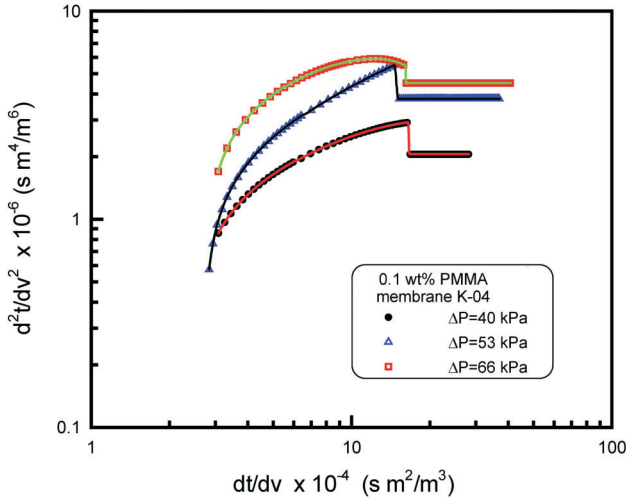

Figure 6. A logarithm plot of d^2t/dv^2 versus dt/dv under various filtration pressures for membrane K-04.

figure can be divided into two segments. It depicts a concave curve before the critical point C and then changes to a straight line after the critical point. According to Eq. (1), one can figure out that the membrane blockings are significant at the first stage, while the cake filtration model can be employed in the second stage. The bend of the curves is doubtless due to the occurrence of membrane pore blocking. Since the reciprocal of dt/dv is equal to the filtration flux, q, Figure 5 also reveals that the filtration flux decreases with the increase of filtration pressure. In addition, to compare the first segment of those curves shown in Figure 5, the deviation from linearity increases with increasing filtration pressure. This implies that the membrane pore blocking is more significant under a higher pressure. It can be also seen that the critical point occurs at greater volume of water filtered as filtration pressure decreases. Since the particle mass flux arriving at the membrane surface can be calculated by the product of suspension concentration and the filtrate volume, cv, larger v value represents more particles being transported to the membrane surface. Therefore, the transition from membrane internal fouling (membrane blocking) to cake filtration needs more particle accumulation in the membrane pores when the filtration pressure is lower.

The filtration data are re-plotted to d^2t/dv^2 versus dt/dv in Figure 6. Each curve can be divided into two distinct parts, an increasing- d^2t/dv^2 part and a constant-d^2t/dv^2 part. According to Eq.(1), the slope of local tangent can be considered as the instantaneous blocking index i. Thus, the values of i decrease continuously in the first part during a filtration instead of four fixed numbers proposed by Hermia [4]. It is possible due to the mixed modes of membrane blocking occurring simultaneously. This phenomenon is the same as those in previous studies [5,6]. Larger variations in the tangent slope of the curves can be found under $\Delta P = 53$ and 66 kPa. This reveals that i changes significantly before the critical point under higher filtration pressures. In the second part, the slope of the tangent suddenly drops to zero at the critical point. Therefore, the filtration follows the cake filtration mode, i.e., $i = 0$.

According to the analysis in the authors' previous study [9], the membrane blocking is affected by two major factors, the particle accumulation and instantaneous filtration flux. A particle may have more opportunity to migrate into the membrane pores in the condition of higher filtration flux because of higher resultant drag or less particle accumulation because of less hindered effect. In order to understand how these factors affecting the membrane blocking in the submerged membrane filtration, the blocking index i under various values of $1/q$ and cv are plotted and discussed in Figures 7 and 8. The effect of $1/q$ on the blocking index, i, under various filtration pressures is shown in Figure 7. Since the pores of a "relative clean membrane" are more easily blocked, the value of $i > 0$ and decreases quickly at the initial periods. When the value of $1/q$ reaches a critical point C, the coming particles will deposit on the membrane surface to

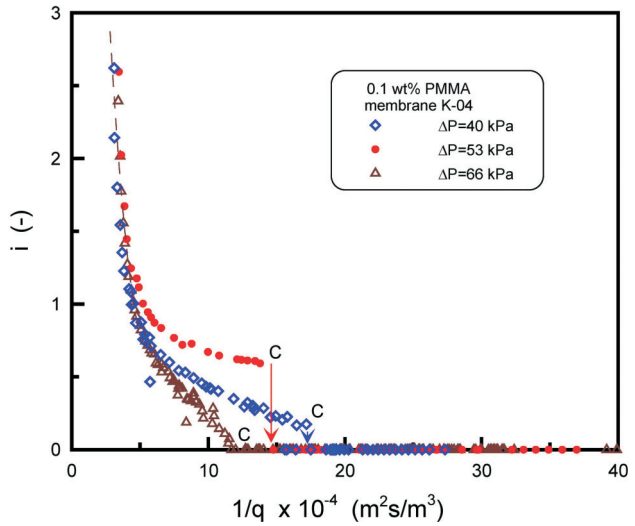

Figure 7. A plot of blocking index versus 1/q under three different filtration pressures for membrane K-04.

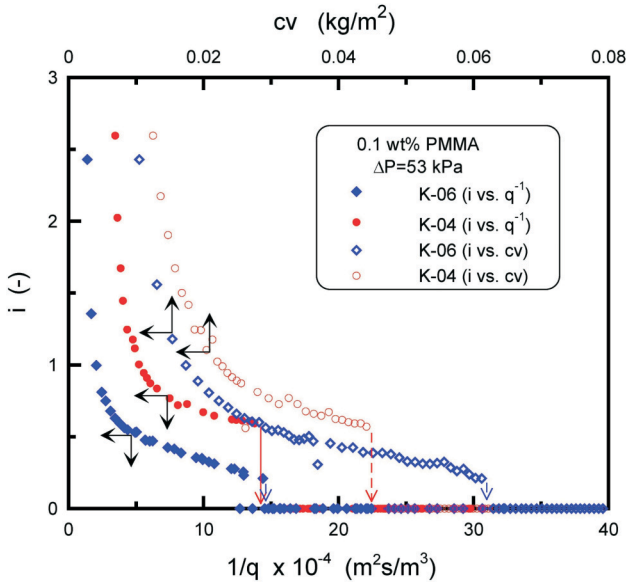

Figure 8. Effects of particle accumulation and filtration flux on the blocking index during the filtration using two kinds of membranes.

form a filter cake causing by the "bridging effect", and the blocking index drops to zero. Comparing the curves shown in Figure 7, the variations of i under different filtration pressures are nearly the same when $1/q < 5 \times 10^4$ m^2s/m^3. This implies that their blocking modes are similar under higher filtration flux. However, the influence of filtration flux becomes more significant as particle accumulation increases. This effect leads the cake filtration mode to earlier occur under higher filtration pressure.

Figure 8 shows the comparisons of blocking index, i, under various filtration fluxes and particle accumulations for two kinds of ceramic membranes. The filtration pressures were kept at 53 kPa during these filtration. The blocking index decreases quickly in the early period of filtration, decreases gradually when the index is smaller than 1.0, and finally, drops to zero at the critical point. Comparing the curves shown in Figure 8, the blocking index for K-04 is always greater than for K-06 for a given filtration flux as well as for a given particle accumulation. This result is attributed to more large pores for membrane K-04; the larger pore size leads no doubt to a more severe membrane blocking. The data also show that more particles accumulate before the critical point for membrane K-06. This is because the pore size distribution of membrane K-06 is a little wider and its internal porosity is higher. Therefore, more particles can be held up in the larger pores of membrane K-06. Moreover, the filtration mode changes to the cake filtration under almost the same filtration flux for two membranes. This implies that the force dragging a particle into the pores of membranes constructed from the same material may be the same. Based on the above analyses, the effects of filtration flux and particle accumulation on the membrane blocking should be considered simultaneously in order to grasp the filtration characteristics.

According to previous analyses, the critical condition changing from membrane blocking to cake filtration mode can be obtained. Figure 9 shows the critical condi-

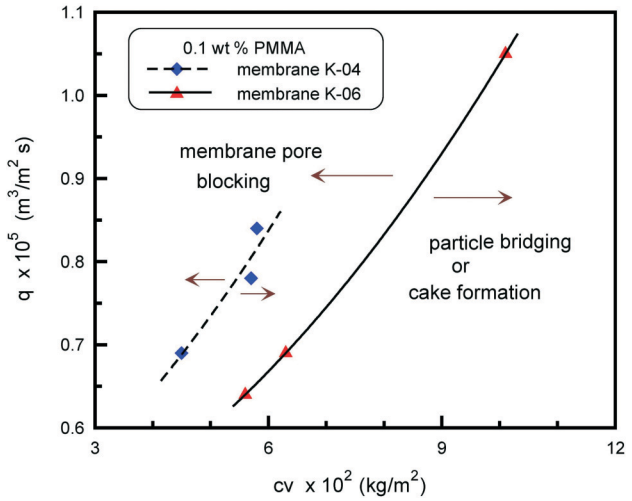

Figure 9. The relationships between q and cv at critical conditions for two membranes.

tions obtained under various pressures for two ceramic membranes. The regressed curves can then be considered as the boundary between membrane pore blocking and particle bridging (cake formation) conditions. Membrane pore blocking occurs in the left-hand-side region, while a filter cake is formed on the membrane surface in the right-hand-side region of the regressed curves. A particle has opportunity to block the membrane pores only under a higher filtration flux (larger drag force) or less particle accumulation (less hindered effect). When particle accumulation increases and filtration flux attenuates beyond the boundary, the filtration follows the cake filtration model. Comparing the critical conditions of the membranes, the boundary for membrane K-04 locates on the left-hand-side to that for membrane K-06. This means that the change to cake filtration occurs at a higher filtration flux or a less particle accumulation when membrane K-04 is used. Since the critical conditions for a given sample can be obtained by the blocking analysis, the results of this method can be provided as guidelines for operations. For example, to keep a lower filtration flux at the initial stage of filtration to avoid a severe membrane blockage may be an efficient way to enhance the filtration efficiency.

The major resistance sources in most microfiltration include the membrane internal fouling, R_{if}, the filter cake, R_c, and the clean membrane, R_m. According to the basic filtration equation, the overall filtration resistance can be expressed as:

$$R_t = R_{if} + R_c + R_m = \frac{\Delta P}{\mu q} \tag{2}$$

Therefore, the overall filtration resistance can be calculated from the experimental data of filtration pressure and filtration flux. Since the resistance of clean membrane can be obtained by pure water flux, the value of R_{if} can be calculated by subtracting R_m from the overall filtration resistance before the critical condition. When a filter cake begins to form at the critical condition, no any more membrane blocking is assumed. Any increase in overall filtration resistance is then attributed to the cake formation. Hence, the value of R_c can be calculated by subtracting R_m and the value of R_{if} at the critical point from the overall filtration resistance.

Figure 10 shows comparisons of R_{if} and R_c under two different filtration pressures. The membrane used in these experiments is membrane K-06. Since the membrane blocking occurs at the initial period of filtration, the value of R_{if} increases with time until the critical point. The filtration then suddenly changes to the cake filtration mode at that point. Hence, the cake resistance increases continuously, while the value of R_{if} maintains constant from the critical point. To compare the curves shown in Figure 10, the values of R_{if} and R_c are higher under a higher pressure. This indicates that more severe membrane internal blocking and more particle fouling on the membrane surface occurs under a higher pressure. A 50% increase in filtration pressure makes a two-fold increase in the filtration resistances. Therefore, when PMMA particles are filtered by these ceramic membranes, a higher pressure leads to a lower filtration flux due to the higher overall filtration resistance, as shown in Figure 4. Furthermore, the results shown in Figure 10 also indicate that the value of R_c becomes comparable with R_{if} at ca 10,000 seconds. In a word, the role of R_{if} is dominant before 4,000 s; R_c increases continuously its importance after 4,000 s and becomes the major after 10,000 s.

The values of R_{if} and R_c can also be measured in experiments. When an experiment is terminated, the overall filtration resistance is calculated, and the membrane is taken out and the cake is washed away by de-ionized water. Then, the residue filtration resistances for the membrane are R_{if} and R_m after washing, and can be measured by pure water flux under the same pressure. The value of

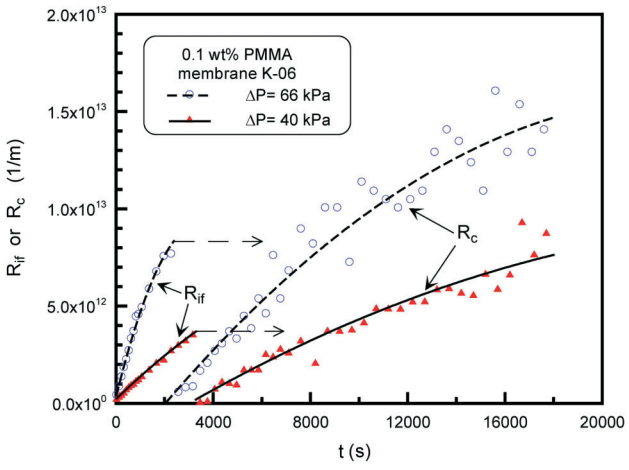

Figure 10. Effect of filtration pressure on the filtration resistances due to membrane blocking and cake formation for membrane K-06.

R_c is obtained by subtracting all the other resistances from R_t. The experimental data of R_{if} and R_c under two filtration pressures for membrane K-06 at 18,000 s are plotted in Figure 11. The values calculated by the method described previously at the same filtration time are also shown for comparison. It can be found that the calculated values of R_{if} are slightly lower than experimental data. This is possible due to the assumption of constant R_{if} after the critical point. In fact, the foulant may migrate in the membrane pores during filtration. However, a deviation less than 10% can be found. On the contrary, the underestimation on R_{if} makes slight higher values of R_c, but the deviation is also reasonable and acceptable. In conclusion, the calculated values of filtration resistances agree well with the experimental data. The proposed method can be used for interpreting the particle fouling in submerged membrane filtration.

Figure 12 depicts the variations of R_{if} and R_c during the filtration using different membranes under the same filtration pressure. The value of R_{if} is higher for membrane K-04 due to more severe membrane blocking, which has been discussed in Figure 8. The filtration changes to cake filtration modes at 3,800 s for membrane K-6; however, the membrane blocking still occurs until 5,400 s for membrane K-04. This leads the value of R_{if} for membrane K-04 to be about two-fold higher than that for membrane K-06. Since the higher resistance and lower filtration flux may retard the particle flux transported to the membrane surface, the value of R_c for membrane K-04 increases much slower than membrane K-06 after the critical point. Furthermore, the sum of R_{if} and R_c for membrane K-06 is lower than that for membrane K-04 at 10,000 s. This makes the filtration flux for membrane K-06 is higher, as shown in Figure 4. However, the cake resistance for membrane K-06 increases more quickly, as a result, the sum of R_{if} and R_c for membrane K-06 becomes higher at 18,000 s. Therefore, a lower flux is obtained for membrane K-06 for a long time operation.

4. Conclusion

The particle fouling in a submerged membrane filtration system has been analyzed using blocking models. Two kinds of ceramic membranes made of ZrO_2-TiO_2 were used for filtering 5 μm PMMA spherical particles. Membranes K-04 and K-06 had mean pore sizes of 8 and 5 μm, respectively, on the outer surfaces. The membrane blocking was dominant at the initial period of a filtration, while the filtration changed to the cake filtration model at a critical condition. The critical conditions obtained by blocking index analysis indicated that membrane blocking occurred under a higher filtration flux or less particle accumulation. Since the resistances due to membrane blocking and to cake formation increased with the increase of filtration pressure for the used membranes, an increase in filtration pressure contrarily led to a lower filtration flux. To compare the used ceramic membranes, membrane K-04 had more severe membrane blocking

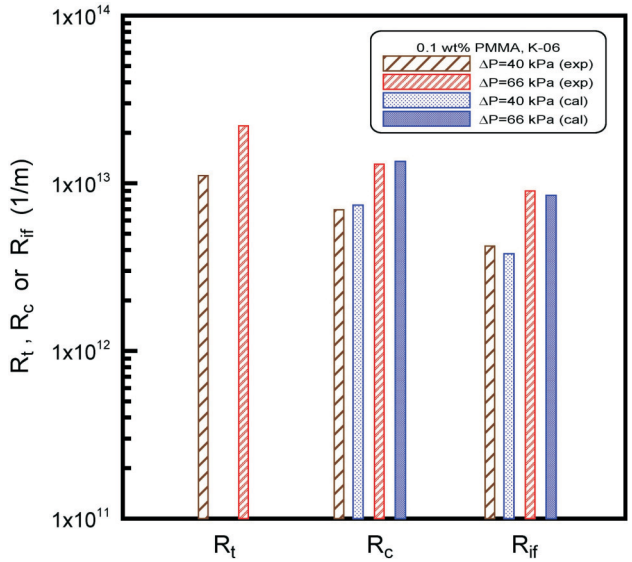

Figure 11. Comparisons of filtration resistances between calculated results and experimental data.

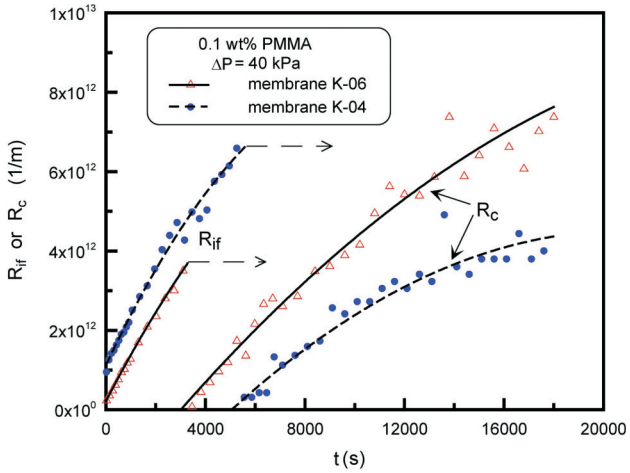

Figure 12. Variations of filtration resistances during constant pressure filtration using two different membranes.

because of more large nominal pores. This fact resulted in a higher resistance and lower flux for membrane K-04 before t = 10,000 s. However, the quicker increase in the cake resistance caused the flux for membrane K-06 became lower at t = 18,000 s. The calculated values of filtration resistances agreed well with the experimental data. This demonstrated that the blocking model analysis could be employed to interpret the particle fouling in submerged membrane filtration.

Acknowledgement

The authors wish to express their sincere gratitude to the National Science Council of the Republic of China for its financial support.

Nomenclature

c particle concentration in suspension (kg/m^2)
i index of blocking model (-)
K resistance coefficient defined in Eq. (1) (s^{1-i}/m^{2-i})
ΔP filtration pressure (N/m^2)
q filtration flux (m^3/m^2 s)
q_s filtration flux at 10000 s (m^3/m^2 s)
R_c resistance of the filter cake (m^{-1})
R_{if} resistance due to internal fouling in the membrane (m^{-1})
R_m resistance of the filter membrane (m^{-1})
R_t overall filtration resistance (m^{-1})
t filtrate time (s)
v filtrate volume per unit filtration area (m^3/m^2)

Greek letters

μ viscosity of fluid (kg/s m)

References

[1] Cheryan, M., *Ultrafiltration and Microfiltration Handbook*, pp. 113–130, Technomic Publishing Co., Pennsylvania, USA (1998).

[2] Belfort, G., Davis, R. H. and Zydney, A. L., "The Behavior of Suspensions and Macromolecular Solutions in Crossflow Microfiltration," *J. Membr. Sci.,* Vol. 96, pp. 1–58 (1994).

[3] Lu, W. M. and Hwang, K. J., "Cake Formation in 2-D Cross-Flow Filtration," *A.I.Ch.E. J.*, Vol. 41, pp. 1443–1455 (1995).

[4] Hermia, J., "Constant Pressure Blocking Filtration Law: Application to Power-Law Non-Newtonian Fluid," *Trans. Inst. Chem. Eng.,* Vol. 60, pp. 183–187 (1982).

[5] Ho, C. C. and Zydney, A. L., "Effect of Membrane Morphology on the Initial Rate of Protein Fouling during Microfiltration," *J. Membr. Sci.,* Vol. 155, pp. 261–275 (1999).

[6] Hwang, K. J. and Lin, T. T., "Effect of Morphology of Polymeric Membrane on the Performance of Cross-Flow Microfiltration," *J. Membr. Sci.,* Vol. 199, pp. 41–52 (2002).

[7] Iritani, E., Katagiri, N., Sugiyama, Y. and Yagishita, K., "Analysis of Flux Decline Behaviors in Filtration of Very Dilute Suspensions," *A.I.Ch.E. J.,* Vol. 53, pp. 2275–2283 (2007).

[8] Ho, C. C. and Zydney, A. L., "A Combined Pore Blockage and Cake Filtration Model for Protein Fouling during Microfiltration," *J. Colloid Interface Sci.,* Vol. 232, pp. 389–399 (2000).

[9] Hwang, K. J., Liao, C. Y. and Tung, K. L., "Analysis of Particle Fouling during Microfiltration by Use of Blocking Models," *J. Membr. Sci.,* Vol. 287, pp. 287–293 (2007).

Manuscript Received: Nov. 21, 2007
Accepted: Oct. 22, 2008